Chemical Methodologies 6(2022) 790-800

Chemical Methodologies

Journal homepage: http://chemmethod.com

Original Research Article

Sensing of Lomustine Drug by Pure and Doped C_{48} Nanoclusters: DFT Calculations

Elnaz Golipour-Chobar, Farshid Salimi*, Gholamreza Ebrahimzadeh-Rajaei

Department of Chemistry, Ardabil Branch, Islamic Azad University, Ardabil, Iran

ARTICLE INFO

Article history

Submitted: 2022-05-30
Revised: 2022-06-02
Accepted: 2022-07-17
Manuscript ID: CHEMM-2205-1555
Checked for Plagiarism: **Yes**
Language Editor:
Dr. Fatimah Ramezani
Editor who approved publication:
Dr. Mohsen Oftadeh

DOI:10.22034/CHEMM.2022.344895.1555

KEYWORDS

Lomustine
Density functional theory
C_{48} nanocluster
Detection
Adsorption

ABSTRACT

Interaction of lomustine with pure C_{48} and Al-, Si-, Ge-, and Ga-doped C_{47} nanoclusters was reviewed. The calculation was done using density functional theory (DFT) with the GAMESS software to find an efficient sensor for lomustine detection. The adsorption energy of pure C_{48} was about -3.35 kcal mol^{-1}. The results indicated weak interaction and sensitivity in the lomustine/C_{48} complex. In addition, lomustine was adsorbed on the Si-, Al-, Ge-, and Ga-doped C_{47} nanoclusters. Thermodynamic calculations were shown the interaction between lomustine and Si-, Al-, Ge-, and Ga-doped C_{47} are spontaneous and exothermic. Although Si-, Al-, Ge-, and Ga-doped C_{47} demonstrated strong adsorption, only sensitivity increased in Al-doped C_{47} (reduced from 1.80 eV in Al-doped C_{47} to 0.75 eV in complex form). Furthermore, Al-doped C_{47} showed a convenient short recovery time. It was concluded that the Al-doped C_{47} nanocluster is a good candidate for identifying lomustine drug.

GRAPHICAL ABSTRACT

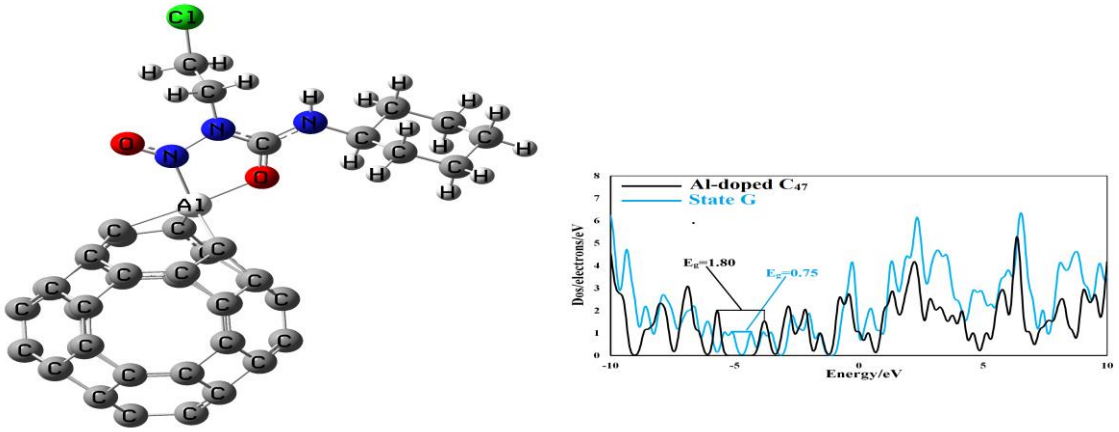

* Corresponding author: , Farshid Salimi
✉ E-mail: Salimi982020@gmail.com

Introduction

Lomustine drug is an alkylating nitrosourea utilized to treat different kinds of cancer [1]. However, its clinical utility is limited by dose-dependent toxicity, such as pulmonary and hematologic toxicity [2, 3]. Furthermore, since lomustine has a hydrophobic structure, intravenous injection is associated with significant side effects like blood respiratory system failure and vessels embolization [4]. Therefore, a rapid and reliable lomustine detection technique is essential.

Chromatographic and spectrophotometric techniques are generally time-consuming, expensive, and more complicated. Besides these, it has been specified that chemical sensors based on nanostructures can detect various materials at low concentrations because of the high surface/volume ratio [5-7]. The utilization of sensors has many advantages, such as easy construction against the easy analytical instrument, short reply time, small size, and low cost [8]. Various nanomaterials like nanocone, nanotubes, nanowires, nanosheets, and nanoclusters have been widely used for chemical sensors [9-17].

Among various nanostructures, fullerenes are known as suitable candidates for chemical sensors of different compounds regarding their appropriate properties such as unique spherical structure, highly symmetrical nature, and hydrophobic characteristics [18-22]. Kroto et al. introduced fullerene (C_{60}) in 1985 [23]. After introducing fullerene C_{60}, the stability and structure of nanoclusters (fullerenes) with less than 60 carbon atoms have attracted considerable attention [24-26]. Different sizes of fullerenes such as C_6, C_{12}, C_{24}, and C_{48} were common resources for chemical sensors and diverse medical applications [27, 28]. Among various sizes of fullerenes studied, the C_{48} nanocluster has gained special attention due to its possible structure flexibility [29, 30]. Therefore, in the current work, the interaction of lomustine with the C_{48} nanocluster was initially investigated using density functional theory (DFT) calculations. Moreover, we inserted Al, Si, Ge, and Ga atoms instead of a C atom in the C_{48} (Al-, Si-, Ge-, and Ga-doped C_{47}) to find an efficient sensor for lomustine detection.

Computational Method

Adsorption of lomustine onto the pure C_{48} and Si-, Al-, Ge-, and Ga-doped C_{47} nanoclusters surface was calculated using DFT. All calculations were done with the GAMESS software [31] with the B3PW91/6-311G(d, p) level of theory [32, 33]. The previous studies were reported that the B3PW91 method is one of the best methods [34, 35], and 6-311G(d, p) basis set known as convenient for nanocarrier systems [36, 37]. The adsorption energies (E_{ad}) of lomustine onto the pure and doped carbon nanoclusters were obtained with the following equations:

$$E_{ad} = E(\text{lomustine}/C_{48}) - E(C_{48}) - E(\text{lomustine}) \quad (1)$$

$$E_{ad} = E(\text{lomustine/Si-doped } C_{47}) - E(\text{Si-doped } C_{47}) - E(\text{lomustine}) \quad (2)$$

$$E_{ad} = E(\text{lomustine/Al-doped } C_{47}) - E(\text{Al-doped } C_{47}) - E(\text{lomustine}) \quad (3)$$

$$E_{ad} = E(\text{lomustine/Ge-doped } C_{47}) - E(\text{Ge-doped } C_{47}) - E(\text{lomustine}) \quad (4)$$

$$E_{ad} = E(\text{lomustine/Ga-doped } C_{47}) - E(\text{Ga-doped } C_{47}) - E(\text{lomustine}) \quad (5)$$

Where E(lomustine/C_{48}), E(lomustine/Si-doped C_{47}), E(lomustine/Al-doped C_{47}), E(lomustine/Ge-doped C_{47}), and E(lomustine/Ga-doped C_{47}) are the total energies of the C_{48}, Si-, Al-, Ge-, and Ga-doped C_{47} interacted with lomustine, and E(lomustine), E(C_{48}), E(Si-doped C_{47}), E(Al-doped C_{47}), E(Ge-doped C_{47}), and E(Ga-doped C_{47}) are the total energy of the lone lomustine, C_{48}, Si-, Al-, Ge-, and Ga-doped C_{47}, respectively. Thermodynamic parameters (enthalpy (ΔH), entropy (ΔS), and Gibbs free energy (ΔG)) were further investigated at the same method to check the validity of the optimization. Moreover, the density of states (DOS), molecular electrostatic potential (MEP), natural bond orbital (NBO), and all energy calculations analyses were reviewed.

Results and Discussion

Adsorption of lomustine onto the C_{48}

The lomustine optimized structure and molecular electrostatic potential (MEP) plot were indicated in Figure 1. As indicated in the MEP plot of lomustine, the negative charges are mainly localized at the 10 and 20 atoms (red color), which can be adsorbed on the electron-withdrawing parts of the nanoclusters [38].

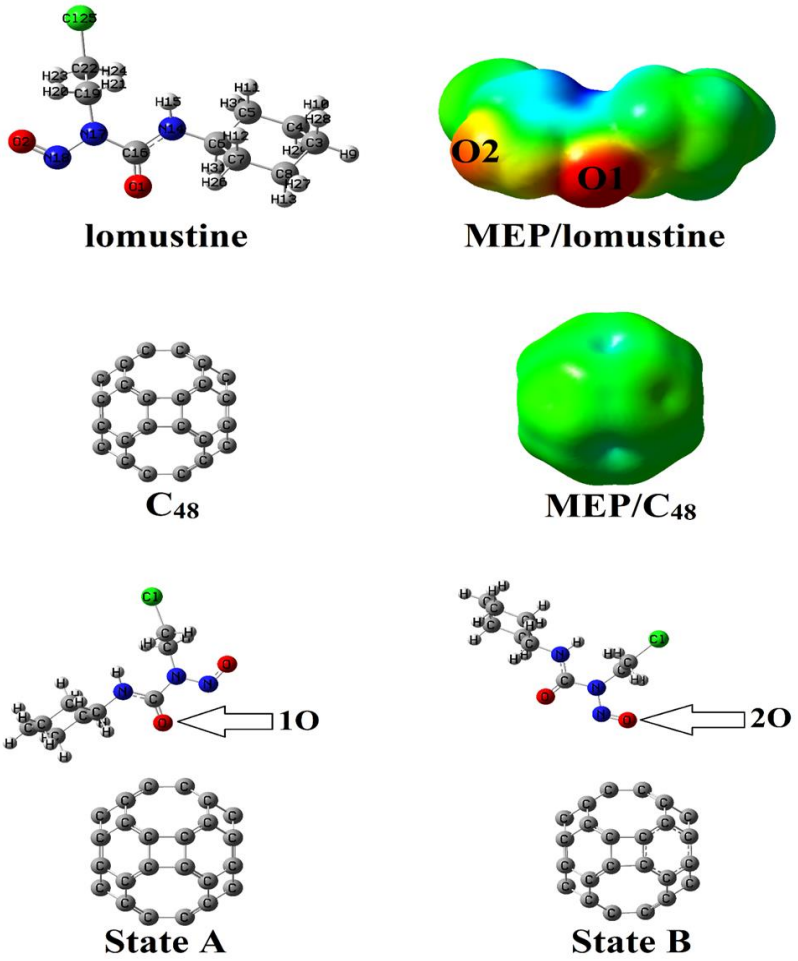

Figure 1: Optimized structure and MEP plots of the letrozole drug and C_{47} and the most stable complexes in states A and B

The optimized nanocluster of C_{48} includes four 4-membered (4-R), four 6-membered (6-R), and two 8-membered (8-R) rings displayed in Figure 1. The angles in C-C-C bounds for octagons is 134.99, for hexagons is 120.01 and for tetragons is 90.01. The C_{48} nanocluster structural properties indicated that three C-C bonds with a bond distance of 1.46, 1.36, and 1.50 Å are correlated to the 6R-4R, 6R-8R, and 4R-8R mutual bonds, respectively, which completely agrees with the previous work [39]. First, the C_{48} nanocluster was selected to investigate the adsorption of lomustine. The reactivity of lomustine with C_{48} was reviewed in diverse adsorption sites (Figure 1). After relaxation, two main orientations were found judging from the values of the thermodynamic calculation and E_{ad} (10 and 20 atoms of lomustine and C atom of C_{47} which their names is states A and B), as indicated in Figure 2. The E_{ad} of lomustine with the C_{48} in states A and B were obtained to be -3.05 and -2.99 kcal mol^{-1} with equilibrium distances of 3.41 and 3.69 Å, respectively (Table 1). Thus, the adsorption of the lomustine (from its 10 orientation) on the C_{48} nanocluster (state A) is the most stable complex since E_{ad} values were indicated in state A are more negative than that of state B, and equilibrium distance is shorter

than the state B. The E_{ad} of lomustine with the $B_{24}N_{24}$ nanocluster was calculated -10.73 kcal mol^{-1} [38]. Therefore, the E_{ad} values indicated appropriate binding in the $B_{24}N_{24}$ nanocluster compared with the C_{48} nanocluster. The natural bond orbital (NBO) calculations were depicted charge transfers from the lomustine to the C_{48} in states A and B to be 0.007 and 0.006 e, respectively. Positive values of the NBO charge of lomustine illustrated that the charge transferred from the drug to C_{48}. After lomustine adsorption on the C_{48} nanocluster, the ΔH parameters were investigated about 6.92 and 8.42 kcal mol^{-1}, and the ΔG values were calculated 21.92 and 27.51 kcal mol^{-1} in state A and B, respectively. These results confirmed the E_{ad} values that the lomustine adsorption is stronger in state A.

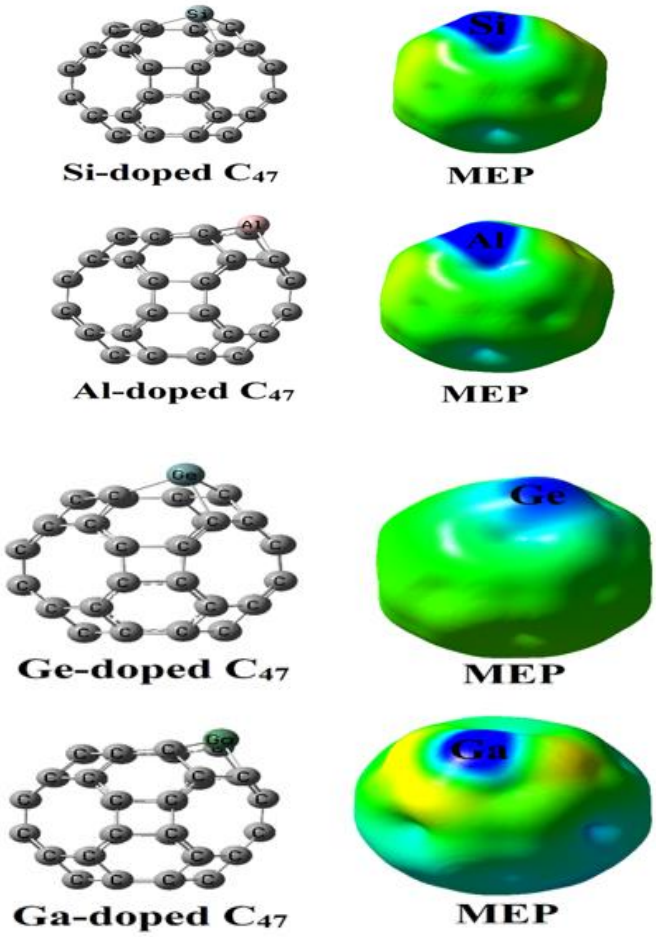

Figure 2: Optimized structures and MEP plots for the Si-, Al-, Ge-, and Ga-doped C_{47}

Adsorption of lomustine onto the Si-, Al-, Ge-, and Ga-doped C_{47}

The E_{ad} of lomustine with C_{48} showed a weak interaction. Thus, a Carbon (C) atom of C_{48} was altered with Silicon (Si), Aluminum (Al), Gallium (Ga), or Germanium (Ge) atom (Si-, Al-, Ga, and Ge-doped C_{47}) for lomustine adsorption. The MEP plots and most stable structures of Si-, Al-, Ga-, and Ge-doped C_{47} are depicted in Figure 2. MEPs of doped nanoclusters revealed Si, Al, Ge, and Ga atoms have more metallic characteristics than the C atoms. The bond length in Si-, Al-, Ge, and Ga-doped C_{47} nanoclusters for doped atoms-C are longer than the corresponding C-C bonds in the C_{48}. The most stable structures of lomustine/ Si-, Al-, Ge, and Ga-doped C_{47} complexes in the two states are demonstrated in Figures 3 and 4. After lomustine adsorption on nanoclusters, the calculated E_{ad} of lomustine/Si-doped C_{47} in states C and D are -67.32 and -24.21 kcal mol^{-1}, and for

lomustine/Ge-doped C_{47} in states E and F are -45.88 and -27.17 kcal mol^{-1}, respectively. Similar to the C_{48}, the lomustine adsorption from its 1O atom with Si-doped C_{47} and Ge-doped C_{47} (states C and E) are the most stable states. When lomustine interacts from its 10 atom with Si and Ge atoms of nanocluster in states C and E (the most stable states), the N-O atoms (2O and 18N) of lomustine are transferred to the carbon atom of the nanoclusters (Figure 3). This decomposition process of the lomustine can destroy drug efficiency. The E_{ad} of lomustine/Al-doped C_{47} and lomustine/Ga-doped C_{47} complexes in states G, H, I, and J was calculated to be -45.00, -32.81, -29.76, and -23.06 kcal mol^{-1}, respectively (Table 1). The equilibrium distances in states G, H, I, and J were determined at 1.93, 1.92, 2.00, and 2.05 Å. The NBO calculation indicated charge transfer from the lomustine to Al- and Ga-doped C_{47} nanoclusters, and values revealed charge transfer in the Al- and Ga-doped C_{47} are more than the pure C_{48}. The ΔH and ΔG values in Al-doped C_{47} and Ga-doped C_{47} nanoclusters were obtained negative values. Thus, negative values indicated that the adsorption of lomustine on the Al-doped C_{47} and Ga-doped C_{47} is exothermic, and the lomustine's adsorption is spontaneous. The E_{ad} calculated values are more negative than the ΔG values, indicating ΔS reduction.

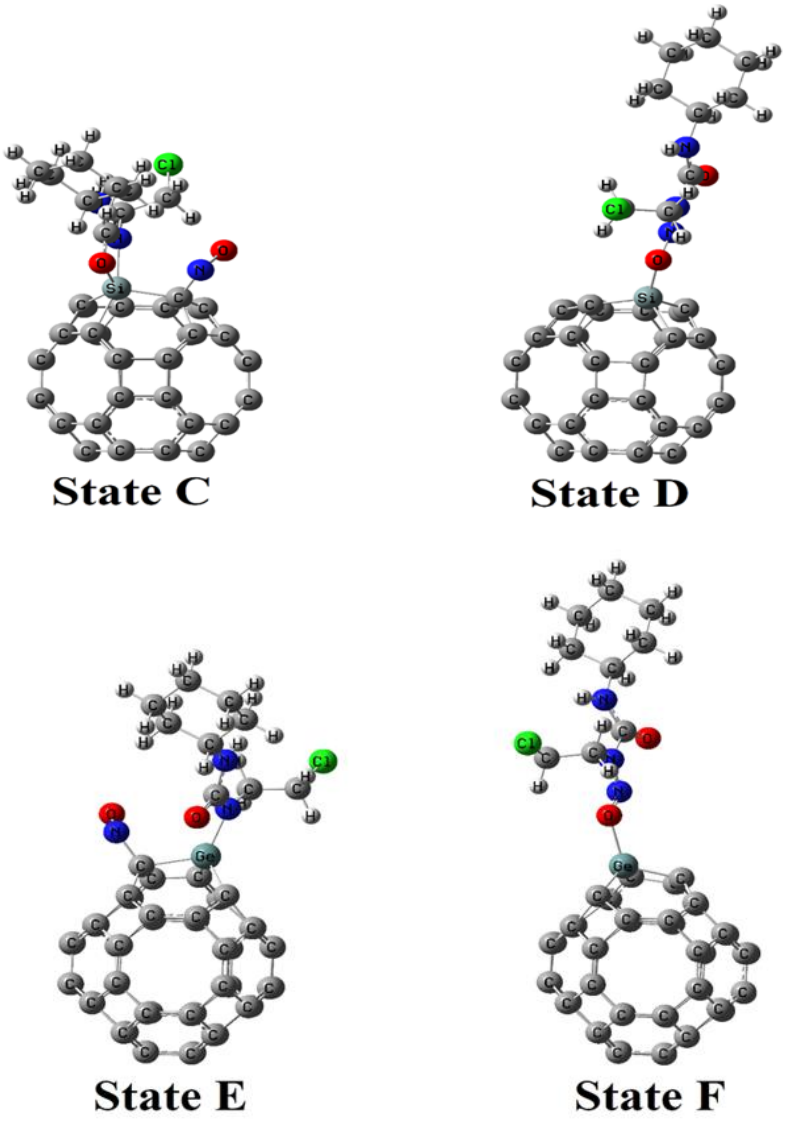

Figure 3: Optimized structures for the Si-doped C_{47} and Ga-doped C_{47} complexes in different states

Table 1: Calculated adsorption energy (Ead/kcal mol-1), bond distance between lomustine and nanoclusters (D/Å), NBO charge on the lomustine in complexes (QNBO/e), HOMO energies (E(HOMO)/eV), LUMO energies (E(LUMO)/eV), energy gap (Eg/eV), and %ΔEg change in electrical conductivity after the lomustine adsorption, dipole moment (DM/Debye), enthalpy (ΔH/kcal mol-1), Gibbs free energy (ΔG/kcal mol-1) and entropy (ΔS/kcal K-1 mol-1), in gas phase

Name	E_{ad}	D	Q_{NBO}	$E_{(HOMO)}$	$E_{(LUMO)}$	E_g	$\%\Delta E_g$	DM	ΔH	ΔG	ΔS
Lomustine	-	-	-	-6.88	-2.04	4.84	-	5.11	-	-	-
C48	-	-	-	-5.59	-4.48	1.11	-	0.00	-	-	-
A	-3.05	3.40	0.007	-5.45	-4.23	1.23	10.81	5.53	6.92	21.92	-0.05
B	-2.99	3.69	0.006	-5.43	-4.21	1.22	9.91	6.52	8.42	27.51	-0.06
Si-doped C_{47}	-	-	-	-5.61	-4.59	1.02	-	1.48	-		0
C	-67.32	1.49	-0.299	-5.22	-4.07	1.15	12.75	8.50	-61.46	-46.59	-0.05
D	-24.21	1.77	0.048	-4.84	-4.20	0.64	-37.25	16.25	-20.17	-12.26	-0.03
Ge-doped C47	-	-	-	-5.59	-4.58	1.02	-	1.85	-		0
E	-45.88	1.48	-0.412	-5.34	-4.15	1.19	16.67	5.93	-39.41	-27.58	-0.04
F	-17.16	1.99	0.150	-4.73	-4.21	0.52	-49.02	19.81	-13.18	-6.15	-0.02
Al-doped C47	-	-	-	-5.69	-3.89	1.80	-	3.33	-		0
G	-45.00	1.93	0.302	-5.09	-4.34	0.75	-58.33	7.39	-38.81	-25.14	-0.05
H	-32.81	1.92	0.164	-4.96	-4.19	0.77	-57.22	20.48	-28.95	-16.27	-0.04
Ga-doped C47	-	-	-	-5.72	-3.94	1.78	-	2.51	-		0
I	-29.76	2.00	0.190	-5.03	-3.48	1.55	-12.92	16.62	-23.58	-15.92	-0.03
J	-23.06	2.05	0.158	-5.03	-3.90	1.13	-36.52	18.96	-19.65	-11.83	-0.03

Evaluation of the electrical properties of lomustine on the nanoclusters

Electronic properties of nanoclusters after and before interaction of the lomustine drug were reviewed in Table 1. In the C_{48} nanocluster, the HOMO and LUMO energies are about -5.59 and -4.48 eV, respectively. Therefore, the E_g (LUMO-HOMO) was calculated at 1.11 eV. Likewise, Kamali *et al*. calculated the E_g of C_{48} 1.11 eV at the same level of theory of the current work [39]. The HOMO and LUMO values changed in the doped nanoclusters. The HOMO energies for Si-, Ge-, Al-, and Ga-doped C_{47} were calculated -5.61, -5.59, -5.69, and -5.79 eV, respectively. Furthermore, LUMO values of Si-, Ge-, Al, and Ga-doped C_{47} were calculated -4.59, -4.58, -3.89, and -3.94 eV, respectively. These results demonstrated that replacing the Si or Ge atoms instead of the C atom stabilizes the HOMO and LUMO levels, and replacing the Al or Ga atoms stabilizes the HOMO and destabilizes the LUMO levels. Therefore, in the Si-, Ge-, Al, and Ga-doped C_{47} nanoclusters, the E_g values were changed 8.11%, 8.11%, -62.16%, and -60.36% compared with the C_{48} nanocluster. After lomustine adsorption, in the most stable complex of the lomustine/C_{48} (state A), the E_g value was not sensibly changed (10.81%). The LUMO and HOMO values in the Si-, Ge-, and Ga-doped C_{47} were altered to higher values after adsorption of lomustine and destabilized the LUMO and HOMO levels. However, in the Al-doped C_{47}, the LUMO value is stabilized by altering from -3.89 to –4.34 eV, and the HOMO value is destabilized by about 0.60 eV. Thus, in the most stable Si-, Ge-, Al- and Ga-doped C_{47} complexes (states C, E, G, and I), the E_g changed about 12.75%, 16.67%, -58.33%, and -12.92%. The E_g values indicate sensitivity and reactivity. The lower levels indicate higher electrical conductivity, sensitivity, and reactivity since the changing in E_g values corresponds to the population of conduction elections, as stated by Equation 6 [40, 41].

$$\sigma = AT^{3/2}\exp(-E_g/2KT) \qquad (6)$$

Where K, A, and T are a constant in Boltzmann's constant, electrons/$m^3.K^{3/2}$, and temperature, respectively. Taking Equation 6 into account, the population of electrical conductivity exponentially increases as E_g decreases, which is changed into an electrical signal. Thus, it is clear that the Al-doped C_{47} is more sensitive than other nanoclusters. Reduce the E_g through the interaction of lomustine revealed the Al-doped C_{47} can sense the lomustine drug. DOS diagram plays a substantial role in the adsorption characteristics of lomustine with the nanoclusters [41-43], as displayed in Figure 5.

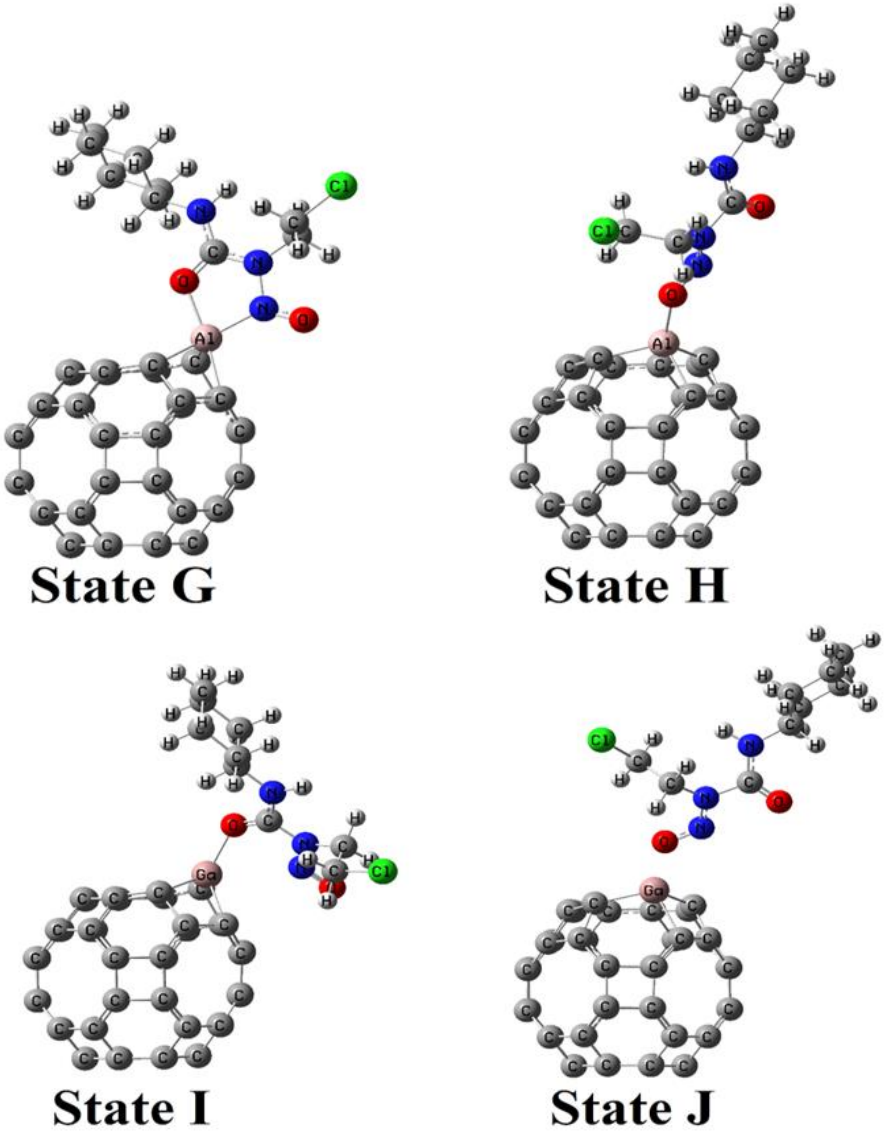

Figure 4: Optimized structures for the Al-doped C_{47} and Ge-doped C_{47} complexes in different states

After the adsorption of lomustine on the Al-doped C_{47}, the DOS plot of the Al-doped C_{47} was changed in the LUMO, HOMO and E_g region. The MEP plots of lomustine/Al-doped C_{47} in the state G (the most stable state) in Figure 5 demonstrate a considerable change after adsorption in the electrostatic potential. The MEP plot was revealed that the lomustine drug is more positive after interaction with nanocluster (blue and green colors). Therefore, this result indicated charge transfers from lomustine to the Al-doped C_{47}, and it could be corroborated the result of NBO charge transfers.

Recovery time

The kind of recovery time and interaction is significant for sensor development. Since strong interactions often cause long recovery times,

which are not suitable for the detection process. The recovery time is recognized experimentally by exposure to the UV light or heating the adsorbent to higher temperatures [44]. Hence, the recovery time was calculated with the following equations:

$$\tau = \upsilon_0^{-1} \exp(-\Delta G/KT) \quad (7)$$

Where T, K, and ν_0 are the temperature, Boltzmann's constant, and attempt frequency, respectively. If UV of 10^{18} s^{-1} ($\nu \sim 10^{18}$ s^{-1}) is used for attempt frequency to extract the lomustine attached to Al-doped C_{47} nanocluster, the recovery time for the lomustine/Al-doped C_{47} will be about 2.58 s at 298 K. These results revealed that the Al-doped C_{47} has an ideal short recovery time. Therefore, the Al-doped C_{47} nanocluster is an appropriate candidate for sensing the lomustine drug.

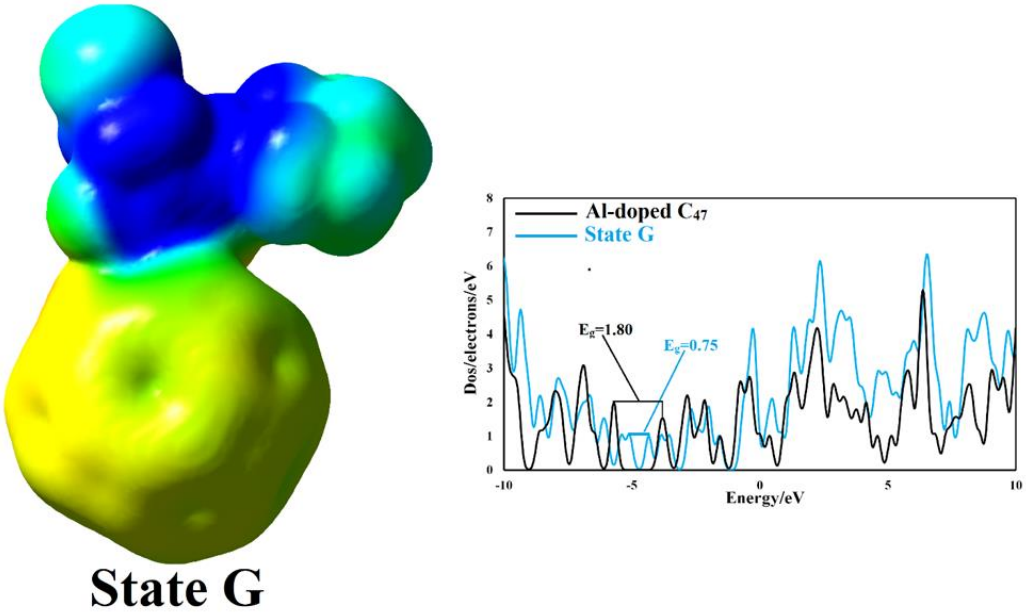

Figure 5: DOS and MEP plots of lomustine/Al-doped C_{47} (state G)

Adsorption of lomustine in the solvent phase

To review the solvent effect on the adsorption process of lomustine on the Al-doped C_{47} nanocluster, the pure nanocluster and most stable complex optimized with taking water as a solvent by using the B3PW91/6-311G(d, p) level of theory. The calculated ΔE_{solv} (total energy in aqua phase - total energy in gas phase) was -11.19 and 20.48 kcal mol^{-1} in the pure and complex form of Al-doped C_{47}, respectively. Therefore, the stability of the structures in the solution phase is significantly enhanced, and the high solvation energies exert their applicability as sensors in biological fluids. The E_{ad} values in the solvent phase were revealed no significant alterations in comparison with the gas phase.

Conclusion

In this work, the adsorption of lomustine on the pure C_{48} and Si-, Al-, Ge-, and Ga-doped C_{47} nanoclusters was reviewed to find a new system for detecting lomustine. The E_{ad} values between lomustine and pure C_{48} nanocluster showed a weak interaction. Lomustine adsorption on the Si- and Ge-doped C_{47} nanoclusters indicated strong interaction, which can decompose the drug. The investigations indicated the appropriate E_{ad} after lomustine adsorbed on the Al-doped C_{47} nanoclusters. In addition, the DOS plots and electrical conductivity indicated that the Al-doped C_{47} nanocluster has excellent sensitivity to the lomustine compared with the Si, Ge-, Ga-doped C_{47} nanocluster. Furthermore, the Al-doped C_{47} nanocluster indicated an appropriate short recovery time. Thus, the results of this study determined that the Al-doped C_{47}

nanocluster can selectively identify the lomustine drug.

Acknowledgements

This article was derived from PhD degree thesis in the Islamic Azad University-Ardabil branch.

Funding

This research did not receive any specific grant from fundig agencies in the public, commercial, or not-for-profit sectors.

Authors' contributions

All authors contributed to data analysis, drafting, and revising of the paper and agreed to be responsible for all the aspects of this work.

Conflict of Interest

There are no conflicts of interest in this study.

ORCID:

Farshid Salimi
https://www.orcid.org/0000-0003-0715-7388

References

[1]. Fisli H., Bensouilah N., Dhaoui N., Abdaoui M., Effects of solvent, pH and β-cyclodextrin on the fluorescent behaviour of lomustine, *Journal of Inclusion Phenomena and Macrocyclic Chemistry*, 2012, **73**:369 [Crossref], [Google Scholar], [Publisher]

[2]. Carter S.K., Schabel Jr F.M., Broder L.E., Johnston T.P., 1,3-Bis(2-Chloroethyl)-1-Nitrosourea (Bcnu) And Other Nitrosoureas In Cancer Treatment: A Review, *Advances in Cancer Research*, 1973, **16**:273 [Crossref], [Google Scholar], [Publisher]

[3]. Nagahiro S., Yamamoto L.Y., Diksic M., Mitsuka S., Sugimoto S., Feindel W., Neurotoxicity after intracarotid 1,3-Bis(2-chloroethyl)-1-nitrosourea administration in the rat: Hemodynamic changes studied by double-tracer autoradiography, *Neurosurgery*, 1991, **29**:19 [Google Scholar], [Publisher]

[4]. Lukyanov A.N., Torchilin V.P., Micelles from lipid derivatives of water-soluble polymers as delivery systems for poorly soluble drugs, *Advanced Drug Delivery Reviews*, 2004, **56**:1273 [Crossref], [Google Scholar], [Publisher]

[5]. Foroughi M.M., Ranjbar M., Graphene Oxide Doped with PbO Nanoparticles, Synthesis by Microwave Assistant Thermal Decomposition and Investigation of Optical Property, *Journal of Cluster Science*, 2017, **28**:2847 [Crossref], [Google Scholar], [Publisher]

[6]. Kakanakova-Georgieva A., Gueorguiev G.K., Stafström S., Hultman L., Janzén E., AlGaInN metal-organic-chemical-vapor-deposition gas-phase chemistry in hydrogen and nitrogen diluents: First-principles calculations, *Chemical physics letters*, 2006, **431**:346 [Crossref], [Google Scholar], [Publisher]

[7]. Hellgren N., Berlind T., Gueorguiev G.K., Johansson M.P., Stafström S., Hultman L., Fullerene-like B-C-N thin films: A computational and experimental study, *Materials Science and Engineering: B*, 2004, **113**:242 [Crossref], [Google Scholar], [Publisher]

[8]. Potyrailo R.A., Polymeric sensor materials: Toward an alliance of combinatorial and rational design tools?, *Angewandte Chemie International Edition*, 2006, **45**:702 [Crossref], [Google Scholar], [Publisher]

[9]. Peyghan A.A., Rastegar S.F., Hadipour N.L., DFT study of NH3 adsorption on pristine, Ni- and Si-doped graphynes, *Physics Letters A*, 2014, **378**:2184 [Crossref], [Google Scholar], [Publisher]

[10].Pashangpour M., Peyghan A.A., Adsorption of carbon monoxide on the pristine, B- and Al-doped C3N nanosheets, *Journal of Molecular Modeling*, 2015, **21**:116 [Crossref], [Google Scholar], [Publisher]

[11].Rivelino R., Dos Santos R.B., de Brito Mota F., Gueorguiev G.K., Conformational effects on structure, electron states, and raman scattering properties of linear carbon chains terminated by graphene-like pieces, *The Journal of Physical Chemistry C*, 2010, **114**:16367 [Crossref], [Google Scholar], [Publisher]

[12].Chernozatonskii L.A., Carbon nanotube elbow connections and tori, *Physics Letters A*, 1992, **170**:37 [Crossref], [Google Scholar], [Publisher]

[13].Yang D.J., Wang S.G., Zhang Q., Sellin P.J., Chen G., Thermal and electrical transport in multi-walled carbon nanotubes, *Physics Letters A*, 2004, **329**:207 [Crossref], [Google Scholar], [Publisher]
[14].Peyghan A.A., Soleymanabadi H., Amir S., Adsorption of H2S at Stone-Wales defects of graphene-like BC3: A computational study, *Molecular Physics*, 2014, **112**:2737 [Crossref], [Google Scholar], [Publisher]
[15].Mei Y.F., Wu X.L., Shao X.F., Huang G.S., Siu G.G., Formation mechanism of alumina nanotube array, *Physics Letters A*, 2003, **309**:109 [Crossref], [Google Scholar], [Publisher]
[16].Zhevago N.K., Glebov V.I., Channeling of fast charged and neutral particles in nanotubes, *Physics Letters A*, 1998, **250**:360 [Crossref], [Google Scholar], [Publisher]
[17].Hadipour N.L., Ahmadi Peyghan A., Soleymanabadi H., Theoretical study on the Al-doped ZnO nanoclusters for CO chemical sensors, *The Journal of Physical Chemistry C*, 2015, **119**:6398 [Crossref], [Google Scholar], [Publisher]
[18].Meier B., Mamone S., Concistrè M., Alonso-Valdesueiro J., Krachmalnicoff A., Whitby R.J., Levitt M.H., Electrical detection of ortho-para conversion in fullerene-encapsulated water, *Nature Communications*, 2015, **6**:8112 [Crossref], [Google Scholar], [Publisher]
[19].Rather J.A., De Wael K., Fullerene-C60 sensor for ultra-high sensitive detection of bisphenol-A and its treatment by green technology, *Sensors and Actuators, B: Chemical*, 2013, **176**:110 [Crossref], [Google Scholar], [Publisher]
[20].Afreen S., Muthoosamy K., Manickam S., Hashim U., Functionalized fullerene (C60) as a potential nanomediator in the fabrication of highly sensitive biosensors, *Biosensors and Bioelectronics*, 2015, **63**:354 [Crossref], [Google Scholar], [Publisher]
[21].Goyal R.N., Gupta V.K., Bachheti N., Fullerene-C60-modified electrode as a sensitive voltammetric sensor for detection of nandrolone-An anabolic steroid used in doping, *Analytica chimica acta*, 2007, **597**:82 [Crossref], [Google Scholar], [Publisher]
[22].Li M., Wei Y., Zhang G., Wang F., Li M., Soleymanabadi H., A DFT study on the detection of isoniazid drug by pristine, Si and Al doped C70 fullerenes, *Physica E: Low-dimensional Systems and Nanostructures*, 2020, **118**:113878 [Crossref], [Google Scholar], [Publisher]
[23].Kroto H.W., Heath J.R., O'Brien S.C., Curl R.F., Smalley R.E., C60: Buckminsterfullerene, *Nature*, 1985, **318**:162 [Crossref], [Google Scholar], [Publisher]
[24].Smalley R.E., Self-Assembly of the Fullerenes, *Accounts of chemical research*, 1992, **25**:98 [Crossref], [Google Scholar], [Publisher]
[25].Chen Z., Jiao H., Bühl M., Hirsch A., Thiel W., Theoretical investigation into structures and magnetic properties of smaller fullerenes and their heteroanalogues, *Theoretical Chemistry Accounts*, 2001, **106**:352 [Crossref], [Google Scholar], [Publisher]
[26].Zhang C., Xu X., Wu H., Zhang Q., Geometry optimization of Cn (n = 2-30) with genetic algorithm, *Chemical physics letters*, 2002, 364:213 [Crossref], [Google Scholar], [Publisher]
[27].Belenkov E.A., Greshnyakov V.A., Diamond-like phases formed from fullerene-like clusters, *Physics of the Solid State*, 2015, **57**:2331 [Crossref], [Google Scholar], [Publisher]
[28].Rad A.S., Ayub K., Nonlinear optical and electronic properties of Cr-, Ni-, and Ti-substituted C20 fullerenes: A quantum-chemical study, *Materials Research Bulletin*, 2018, **97**:399 [Crossref], [Google Scholar], [Publisher]
[29].Zhang B.L., Wang C.Z., Ho K.M., Xu C.H., Chan C.T., The geometry of small fullerene cages: C20 to C70, *The Journal of Chemical Physics*, 1992, **97**:5007 [Crossref], [Google Scholar], [Publisher]
[30].Wu H.S., Xu X.H., Jiao H., Structure and stability of C48 fullerenes, *The Journal of Physical Chemistry A*, 2004, **108**:3813 [Crossref], [Google Scholar], [Publisher]
[31].Schmidt M.W., Baldridge K.K., Boatz J.A., Elbert S.T., Gordon M.S., Jensen J.H., Koseki S., Matsunaga N., Nguyen K.A., Su S., Windus T.L., Dupuis M., Montgomery, Jr J.A., General atomic and molecular electronic structure system, *Journal of computational chemistry*, 1993, **14**:1347 [Crossref], [Google Scholar], [Publisher]

[32].Perdew J.P., Wang Y., Accurate and simple analytic representation of the electron-gas correlation energy, *Physical Review B*, 1992, **45**:13244 [Google Scholar], [Publisher]
[33].Becke A.D., Density-functional thermochemistry. II. The effect of the Perdew-Wang generalized-gradient correlation correction, *The Journal of Chemical Physics*, 1992, **97**:9173 [Crossref], [Google Scholar], [Publisher]
[34].Su K., Wei J., Hu X., Yue H., Lü L., Wang Y., Wen Z., Systematic Comparison of Geometry Optimization on Inorganic Molecules, *Acta Physico-Chimica Sinica*, 2000, **16**:650 [Google Scholar]
[35].Su K.H., Wei J., Hu X.L., Yue H., Lü L., Wang Y.B., Wen Z.Y., High-level Ab Initio Energy Divergences between Theoretical Optimized and Experimental Geometries, *Acta Physico-Chimica Sinica*, 2000, **16**:722 [Google Scholar]
[36].Kazemi M., Rad A.S., Sulfur mustard gas adsorption on ZnO fullerene-like nanocage: Quantum chemical calculations, *Superlattices Microstruct*, 2017, **106**:122 [Crossref], [Google Scholar], [Publisher]
[37].Deng W.Q., Xu X., W.A. Goddard, New alkali doped pillared carbon materials designed to achieve practical reversible hydrogen storage for transportation, *Physical review letters*, 2004, **92**:166103 [Google Scholar], [Publisher]
[38].Golipour-Chobar E., Salimi F., Ebrahimzadeh Rajaei G., Boron nitride nanocluster as a carrier for lomustine anticancer drug delivery: DFT and thermodynamics studies, *Monatshefte für Chemie-Chemical Monthly*, 2020, **151**:309 [Crossref], [Google Scholar], [Publisher]
[39].Kamali F., Ebrahimzadeh Rajaei G., Mohajeri S., Shamel A., Khodadadi-Moghaddam M., Adsorption behavior of metformin drug on the C60 and C48 nanoclusters: a comparative DFT study, *Monatshefte für Chemie-Chemical Monthly*, 2020, **151**:711 [Crossref], [Google Scholar], [Publisher]
[40].Aihara J.I., Reduced HOMO-LUMO Gap as an Index of Kinetic Stability for Polycyclic Aromatic Hydrocarbons, *The Journal of Physical Chemistry A*, 1999, **103**:7487 [Crossref], [Google Scholar], [Publisher]
[41].Aghaei M., Ramezanitaghartapeh M., Javan M., Hoseininezhad-Namin M.S., Mirzaei H., Rad A.S., Soltani A., Sedighi S., Lup A.N.K., Khori V., Mahon P.J., Heidari F., Investigations of adsorption behavior and anti-inflammatory activity of glycine functionalized Al12N12 and Al12ON11 fullerene-like cages, *Spectrochimica Acta Part A: Molecular and Biomolecular Spectroscopy,* 2021, **246**:119023 [Crossref], [Google Scholar], [Publisher]
[42].Kaloni T.P., Tuning the structural, electronic, and magnetic properties of germanene by the adsorption of 3d transition metal atoms, *The Journal of Physical Chemistry C*, 2014, **118**:25200 [Crossref], [Google Scholar], [Publisher]
[43].Kaloni T.P., Schreckenbach G., Freund M.S., Large enhancement and tunable band gap in silicene by small organic molecule adsorption, *The Journal of Physical Chemistry C*, 2014, **118**:23361 [Crossref], [Google Scholar], [Publisher]
[44].Li J., Lu Y., Ye Q., Cinke M., Han J., Meyyappan M., Carbon nanotube sensors for gas and organic vapor detection, *Nano Letters.*, 2003, **3**:929 [Crossref], [Google Scholar], [Publisher]

HOW TO CITE THIS ARTICLE
Elnaz Golipour-Chobara, Farshid Salimi, Gholamreza Ebrahimzadeh-Rajaei. Sensing of Lomustine Drug by Pure and Doped C48 Nanoclusters: DFT Calculations. *Chem. Methodol.*, 2022, 6(10) 790-800
https://doi.org/10.22034/CHEMM.2022.344895.1555
URL: http://www.chemmethod.com/article_154163.html